Inelastic Scattering form Factors for Carbon and Oxygen Halo Isotopes

Alyaa F. Rajab[1*], Khalid S. Jassim[2]

Abstract

In the present article, an inelastic electron scattering form factors $^{13,15,19}C$ nuclei distributed in the 1p1/2, 1d5/2 and 2s1/2 model space (outside ^{12}C inert core) and $^{17,23}O$ nuclei in sd model space (outside ^{16}O inert core) has been studied. $^{15,19}C$ and ^{23}O is one neutron halo nuclei. The shell model calculations have been completed by the recent version of the shell model code NushellX@MSU. The effective interactions ZBMI employed to calculate the energy eigenvalues and eigen states that is used to calculate the one body transition densities (OBTD) to be used in the inelastic electron scattering form factors calculations. Tassie and Bohr-Mottelson models are employed to calculate the total form factors with harmonic oscillator potential (HO) and we get good agreement with available experimental data.

Key Words: Inelastic Electron Scattering, Nuclear Shell Model, NushellX@MSU Code, One Neutron Halo Nuclei, Total form Factor, Tassie Model, Bohr-Mottelson Model.

DOI Number: 10.14704/nq.2020.18.9.NQ20213 **NeuroQuantology 2020; 18(9):35-39**

Introduction

Electron scattering includes nuclear structural information including charge distribution, size, and currents of the electromagnetic within the nucleus. Since 1929 the theoretical calculations on the electron scattering started [1], when mott obtained the relativistic scattering cross section of the Dirac particles. The nuclear size can be determined by multiplying the cross section of Mott with one factor, which is called the nuclear form factor based on the charge, current and magnetization distribution of the target nucleus. The form factor can be experimentally identified by the knowledge of the energies and scattering of the electron and the scattering angle as a function of the momentum transfer (q) [3]. One of the models that attempted to explain the nuclei's static properties when charges effective are applied is shell model within a given model space. Although the success of the 1p-shell model for static characteristics, the electron scattering data are not explained in this area at high momentum transfer. The model space extending to include the $2\hbar\omega$ Configurations improve agreement with the transverse form factor at the beginning of the p-shell but the situation worsens at the end of the p-shell [4].

Through calculations of the shell model, numerous shell model codes were developed to solve the problem of the eigenvalue, like the OXBASH [5], ANTOINE [6], NUSHELL [7], and NUSHELLX [8].

Corresponding author: Alyaa F. Rajab
Address: [1,2]Department of Physics, College of Education for Pure Science, University of Babylon, Babylon, Iraq.
[1*]E-mail: alyaa.rajab@yahoo.com
Relevant conflicts of interest/financial disclosures: The authors declare that the research was conducted in the absence of any commercial or financial relationships that could be construed as a potential conflict of interest.
Received: 12 July 2020 **Accepted:** 10 August 2020

For more than two decades the Hamiltonian USD [9] Realistic sd-shell functions "0d5/2, 0d3/2, 1s1/2" for use in nuclear spectroscopy, nuclear structure models, and nuclear astrophysics were presented.

It seems to be an important characteristic of the Hamiltonian used for p-sd [10] and sd-pf model spaces [11-14]. The Hamiltonian of USD is created by sixty three of the two-body matrix elements and three energies of the single-particle [15]. Proton-neutron formalism interactions of the USDA include a new Hamiltonian of USD-type, based on a 66-parameter to fit for 608 sd-shell energy data "A=16-40", with root mean square (rms) 130 keV and 170 keV[14] [16], respectively. This newest interaction clearly overcomes the fluorine isotope and other oxygen isotopes problem. The energy of the single particle of USDA effective interaction are "1.9798 MeV, -3.9436 and -3.0612 MeV" for the $0d_{3/2}$, $0d_{5/2}$ and $0d_{1/2}$ orbital. Many authors have been very interested in computing Coulomb form factors with specific model spaces, as in some references. [17] [18]. Other theoretical studies the form factors of the electron scattering for light nuclei in "psd, sdpf or psd" shells have been performed by K. S. Jassim et. al. [19][20][21][22][23].

Theory

The Bohr-Mottelson collective's microscopic derivation. The quantified Hamiltonian 5D group gives the form follows: [24], [25]

$$\hat{H}_{coll} = \hat{T}_{vib} + \hat{T}_{rot} + V(\beta,\gamma) \quad (1)$$

Here $\hat{T}_{vib}$, definition of the kinetic vibrational energy [24]

$$\hat{T}_{vib} = -\frac{1}{2D}\left(\frac{1}{\beta^4}\frac{\partial}{\partial\beta}\beta^4\frac{\partial}{\partial\beta} + \frac{1}{\beta^2\sin(3\gamma)}\frac{\partial}{\partial\gamma}\sin(3\gamma)\frac{\partial}{\partial\gamma}\right),$$

and the term of the rotational energy $\hat{T}_{rot}$ is given by [24],

$$\hat{T}_{rot} = \sum_{k=1}^{3}\frac{\hat{I}_k^2}{2\,\mathcal{J}_k(\beta,\gamma)} \quad (2)$$

The classical Hamiltonian (1) is indicated in five curvilinear (β,γ and three Euler angles related by a transformation linear with φ_k) and time derivatives. In coordinates of the curvilinear, we should introduce the so-called Pauli prescription for quantification. The collective equation of Schrödinger [24][25]

$$\left(\hat{T}_{vib} + \hat{T}_{rot} + V(\beta,\gamma)\right)\Psi_{\alpha IM}(\beta,\gamma,\Omega) = E_{\alpha I}\,\Psi_{\alpha IM}(\beta,\gamma,\Omega) \quad (3)$$

Within the laboratory frame the collective wave functions, $\Psi_{\alpha IM}(\beta,\gamma,\Omega)$ is a function of β, γ and α set of three Euler angles Ω and it's specific by the total angular momentum I, its projection onto the z-axis in the laboratory frame M and α that distinguishes the eigen states with the same I and M values. With the wave function of rotational $\mathcal{D}_{MK}^{I}$, they are written as [24][25]

$$\Psi_{\alpha IM}(\beta,\gamma,\Omega) = \sum_{K=even}\Phi_{\alpha IK}(\beta,\gamma)\,\langle\Omega|IMK\rangle, \quad (4)$$

$$\langle\Omega|IMK\rangle = \sqrt{\frac{2I+1}{16\pi^2(1+\delta_{K0})}}\left[\mathcal{D}_{MK}^{I}(\Omega) + (-1)^I\,\mathcal{D}_{M,-K}^{I}(\Omega)\right] \quad (5)$$

Within the body-fixed frame the vibrational wave functions, $\Phi_{\alpha IK}(\beta,\gamma)$, are normalized as [24]:

$$\int d\beta\, d\gamma\,\sqrt{G(\beta,\gamma)}\,|\Phi_{\alpha I}(\beta,\gamma)|^2 = 1\,, \quad (6)$$

Where, $|\Phi_{\alpha I}(\beta,\gamma)|^2 = \sum_{K=even}|\Phi_{\alpha IK}(\beta,\gamma)|^2 \quad (7)$

The volume element is also represented $\sqrt{G(\beta,\gamma)}\,d\beta\,d\gamma$ with

$$G(\beta,\gamma) = 4\,\beta^8\,W(\beta,\gamma)\,R(\beta,\gamma)\sin^2(3\gamma) \quad (8)$$

Comprehensive descriptions of the collective wave functions symmetries and the boundaries conditions of the Schrödinger collective equation solution in Ref. [26-27].

we found the vibrational wave functions of the eigenvalue equation by inserting (4) into the collective Schrödinger equation (3) [24][25]

$$\left[\hat{T}_{vib} + V(\beta,\gamma)\right]\Phi_{\alpha IK}(\beta,\gamma) + \sum_{K'=even}\langle IMK|\hat{T}_{rot}|IMK'\rangle\,\Phi_{\alpha IK'}(\beta,\gamma) = E_{\alpha I}\,\Phi_{\alpha IK}(\beta,\gamma) \quad (9)$$

We get quantum spectrum and collective wave functions by solving this equation. The electromagnetic probabilities of change between collective excited states are then explicitly calculated. The popular multiple decomposition gives the electron scattering form factors

$$F_L^2(q) = \frac{4\pi}{Z^2}\frac{1}{(2J_i+1)}\sum_{J\geq 0}\left|\left\langle J_f\left\|\hat{O}_J^{col.}(q)\right\|J_i\right\rangle\right|^2, \quad (10)$$

where, $T_J^{col.}(q)$ is the operators of the Coulomb multiple.

The matrix element reduced by the desired operator O_Λ^η is represented as the product sum of the one-body matrix density (OBMD) elements times the single-particle matrix elements,

$$\left\langle J_f\left\|\hat{O}_{J,t_z}^{\eta}\right\|J_i\right\rangle = \sum_{c,d} OBMD^{J,t_z}(J_i,J_f,c,d)\left\langle c\left\|\hat{O}_{J,t_z}^{col.}\right\|d\right\rangle,$$

$t_z = \frac{1}{2}$ for a proton and $-\frac{1}{2}$ for a neutron J_i and J_f are initial and final states of the nucleus respectively, and J is the multipolarity. The double bar $\langle \| \rangle$ indicates that the element of the matrix in spin space is reduced.

The states of the single particle are specific by c and d for the final and initial states, respectively [28].

$$|c\rangle = |n_c l_c\rangle |j_c m_c\rangle \quad (12)$$

$$|d\rangle = |n_d l_d\rangle \; |j_d m_d\rangle \;, (13)$$

$$\langle n_c l_c j_c \| \hat{O}_{J,t_z}(q) \| n_d l_d j_d \rangle = e(t_z) \langle n_c l_c | j_J(qr) | n_d l_d \rangle \langle l_c \tfrac{1}{2} j_c \| Y_J(\Omega_r) \| l_d \tfrac{1}{2} j_d \rangle \quad (14)$$

The spherical harmonic reduced matrix elements is,

$$\langle l_c \tfrac{1}{2} j_c \| Y_J(\Omega_r) \| l_d \tfrac{1}{2} j_d \rangle = \frac{1}{2}(-1)^{j_c+\frac{1}{2}}\left[1+(-1)^{l_c+J+l_d}\right]\sqrt{\frac{(2j_c+1)(2j_d+1)(2J+1)}{4\pi}} \begin{pmatrix} j_c & J & j_d \\ 1/2 & 0 & -1/2 \end{pmatrix} \quad (15)$$

The matrix element of the single-particle Bessel's function is [28]:

$$\langle n_c l_c | j_J(qr) | n_d l_d \rangle = \int_0^\infty dr\, r^2\; j_J(qr)\, R_{n_c l_c}(r) R_{n_d l_d}(r),$$

$R_{nl}(r)$ is the radial part of the single-particle wave function. Used a potential of the Harmonic Oscillator HO, characterized by the parameter size. b.

Results and Discussion

The total form factors of ^{13}C, ^{15}C and ^{19}C Isotopes are calculated by using Tassie and Bohr-Mottelson models. These calculations are done using NushellX@MSU computer code. The calculations for the M1, E2 and M3 total form factors with full $1p_{1/2}$, $1d_{3/2}$ and $1s_{1/2}$ model space for angular momentum transfer$(0 < q < 3\ \text{fm}^{-1})$ are performed and compared with the available experimental data.
The total (M1+E2) form factor for the state $5/2^{+}_{1}$ with 3.853 MeV of ^{13}C nucleus as shown in Figure 1. The experimental data for this state are obtained from Ref We need to consider the total contribution of M1 and E2 multipoles. The shell model calculations are performed using ZBMI effective interaction. The red, blue and green curves represent the calculations with model space only (MS), Tassie and Bohr-Mottelson collective models, respectively. It is clear that the total form factor corresponds exactly with the experimental data from the momentum transfer range 1.7 fm^{-1} to 2.5 fm^{-1} in all models.

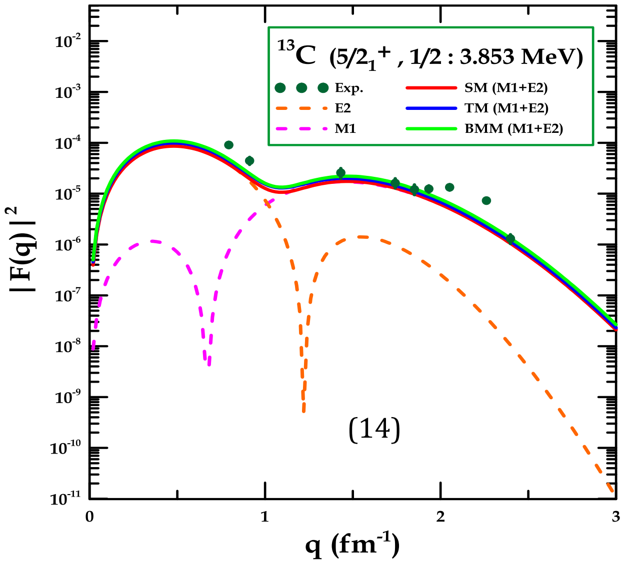

Figure 1. Total M1 and E2 form factor for $5/2^{+}_{1}$ (3.853 MeV) state in the ^{13}C nucleus. Red, blue and green curves represent the calculations model space, Tassie and Bohr-Mottelson models respectively. The experiment data are taken from ref.

Fig.s (2) and (3) are shown the total form factor of E2 and M3 multipoles for the state $(J^{\pi}, T = 5/2^{+}_{1}, -1/2)$ (0.740 MeV) of ^{15}C and $(0.653\ MeV)$ of ^{19}C isotopes, respectively. It is calculated by using ZBMI effective interaction in $1p_{1/2}$, $1d_{3/2}$ and $1s_{1/2}$ model space and assumed ^{12}C isotope as inert core. The red curve act for the Model space (MS) calculations, while, the blue and green curves represent Tassie and Bohr-Mottelson models calculations, respectively. It is apparent that the total form factor agrees significantly with experimental data in the momentum transfer range between $(1.8 < q < 2.1\,)\ \text{fm}^{-1}$ for all models.

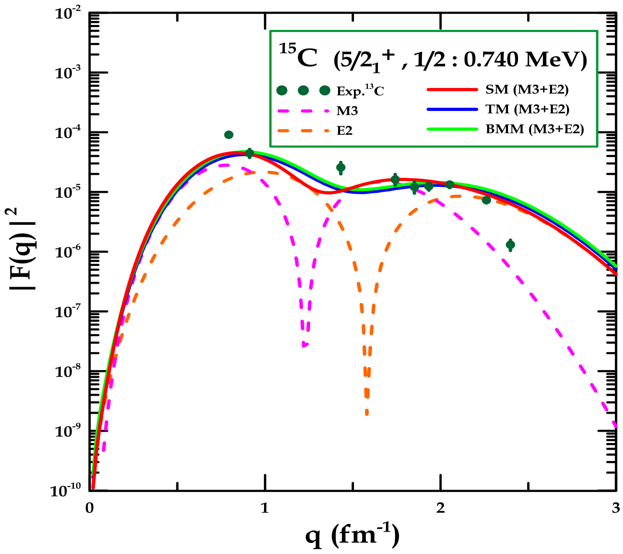

Figure 2. Total E2 and M3 form factor for $5/2^{+}_{1}$ (0.740 MeV) state in the ^{15}C one neutron halo nucleus. Red, blue and green curves represent the calculations using model space (MS) only, Tassie and Bohr-Mottelson models respectively.

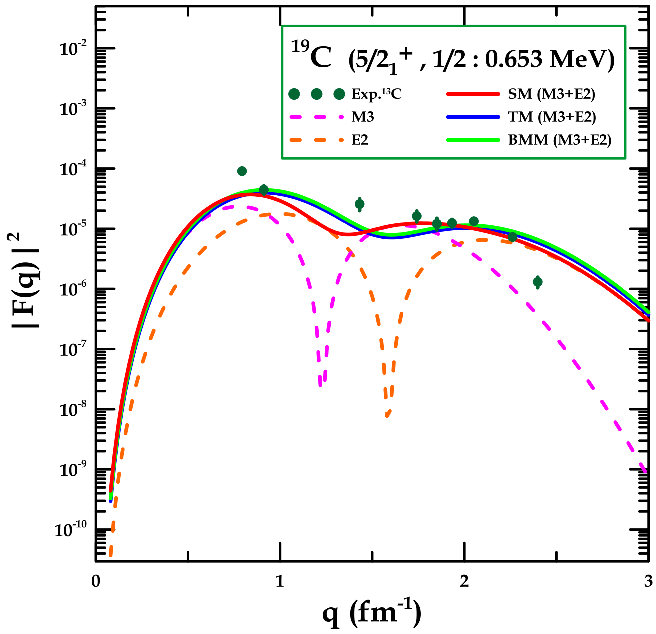

Figure 3. Total E2 and M3 form factor for $5/2_1^+$ (0.367 MeV) state in the ^{19}C one neutron halo nucleus. Red, blue and green curves represent the calculations MS, TM and BMM, respectively.

In Fig. (4), the total form factor of M1, M3 and M5 multipoles for the ground state $1/2^+_1$ of ^{17}O are shown. It is calculated by employing USDA effective interaction in sd model space and assumed ^{16}O isotope as inert core. The red curve represents to shell model calculations; the blue and green curves represent Tassie and Bohr-Mottelson models calculations respectively. TM and BM models give descriptions may be not exact for the experimental data, especially at the momentum transfer after 3.0 fm^{-1}.

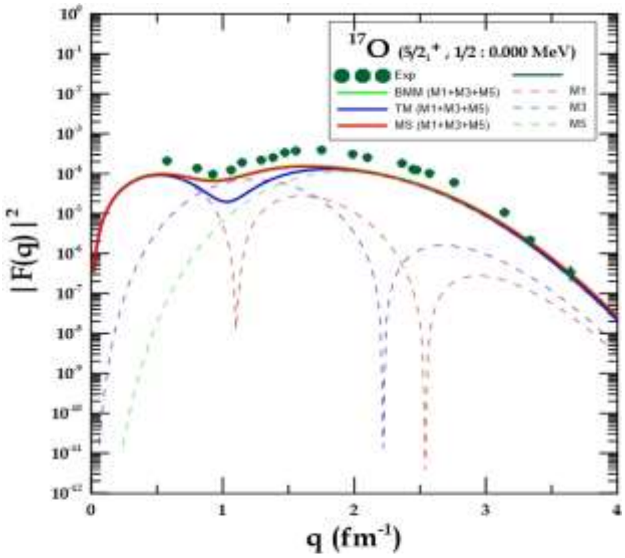

Figure 4. Total M1, M3 and M5 form factor for $5/2_1^+$ (0.000 MeV) state in the ^{17}O nucleus. Red, blue and green curves represent the calculations with MS only, Tassie and Bohr-Mottelson models respectively. Forest green circles represent experiment values which are taken from [29].

Conclusions

The harmonic oscillator potential (HO) is an adequate choice as remaining effective interaction for the form factors calculations with specific effective neutron and proton effective charges. Bohr-Mottelson model and Tassie model are able to reproduce the experimental data and they are well succeed in studying the total nuclear form factor of light nuclei including the one neutron halo.

References

Mott NF. The scattering of fast electrons by atomic nuclei. *Proceedings of the Royal Society of London. Series A, Containing Papers of a Mathematical and Physical Character* 1929; 124(794): 425-442.

Brown BA, Radhi R, Wildenthal BH. Electric quadrupole and hexadecupole nuclear excitations from the perspectives of electron scattering and modern shell-model theory. *Physics Reports* 1983; 101(5): 313–358.

Sagawa H, Brown BA. E2 core polarization for sd-shell single-particle states calculated with a skyrme-type interaction. *Nuclear Physics A* 1984; 430(1): 84–98.

Delorme J, Figureau A, Guichon P. Nuclear critical opalescence and the M1 form factors of 12C and 13C. *Applied Physics Letters B* 1981; 99(3): 187–190.

Etchegoyen A, Rae WD, Godwin NS, Richter WA, Zimmermann CH, Brown BA, Ormand WE, Winfield JS. Program OXBASH, MSU-NSCL Report 524, 1985.

Caurier E, Nowacki F. Present status of shell model techniques. *AcPPB* 1999; 30(3): 705.

Brown BA, Rae WDM. "Nushell@msu" MSU-NSCL report 2007.

Brown BA, Rae WDM.
"NuShellX", http://www.nscl. msu.edu/~brown/resources /resources.html; http://knollhouse.org/default.aspx. 2008.

Wildenthal BH. Empirical strengths of spin operators in nuclei. *Progress in particle and nuclear physics* 1984; 11: 5-51.

Warburton EK, Brown BA. Effective interactions for the 0p1s0d nuclear shell-model space. *Physical Review C* 1992; 46(3): 923–944.
http://doi.org/10.1103/PhysRevC.46.923.

Warburton EK, Becker JA, Brown BA. Mass systematics for A=29-44 nuclei: The deformed a 32 region. *Physical Review C* 1990; 41(3): 1147–1166.
http://doi.org/10.1103/PhysRevC.41.1147.

Utsuno Y, Otsuka T, Mizusaki T, Honma M. Varying shell gap and deformation in N = 20 unstable nuclei studied by the Monte Carlo shell model. *Physical Review C* 1999; 60(5): 54315.
http://doi.org/10.1103/PhysRevC.60.054315.

Nummela S, Baumann P, Caurier E, Dessagne P, Jokinen A, Knipper A, Radivojevic Z. Spectroscopy of 3 4, 3 5 Si by β decay: s d− f p shell gap and single-particle states. *Physical Review C* 2001; 63(4): 044316.
http://doi.org/10.1103/PhysRevC.63.044316.

Brown BA, Richter WA. New ``USD'' Hamiltonians for the sd-shell. *Physical Review C* 2006; 74(3): 34315. http://doi.org/10.1103/PhysRevC.74.034315.

Bertsch G, Borysowicz J, McManus H, Love WG. Interactions for inelastic scattering derived from realistic potentials. *Nuclear Physics A* 1977; 284(3): 399–419.

http://doi.org/10.1016/0375-9474(77)90392-X.

Richter WA, Brown BA. ^{26}Mg observables for the USDA and USDB Hamiltonians. *Physical Review C* 2009; 80(3): 34301.

http://doi.org/10.1103/PhysRevC.80.034301.

Liu J, Zhang J, Xu C, Ren Z. Nuclear longitudinal form factors for axially deformed charge distributions expanded by nonorthogonal basis functions. *Chinese Physics C* 2017; 41(5): 54101.

Liu J, Xu C, Wang S, Ren Z. Coulomb form factors of odd-A nuclei within an axially deformed relativistic mean-field model. *Physical Review C* 2017; 96(3): 34314.

Radhi RA, Hamoudi AK, Jassim KS. Calculations of longitudinal form factors of p-shell nuclei, using enlarged model space including core-polarization effects with realistic two-body effective interaction. *Indian Journal of Physics* 2007; 81(7): 683–695.

Jassim KS, Sahib SR. Large-scale shell model calculations of the 25, 26Mg, 27Al and 19F nucleus. *International Journal of Nuclear Energy Science and Technology* 2018; 12(1): 81-91.

Jassim KS, Al-Sammarrae AA, Sharrad FI, Abu Kassim H. Elastic and inelastic electron-nucleus scattering form factors of some light nuclei: Na 23, Mg 25, Al 27, and Ca 41. *Physical Review C - Nuclear Physical* 2014; 89(1): 014304.

http://doi.org/10.1103/PhysRevC.89.014304.

Jassim KS, Radhi RA, Hussain NM. Inelastic magnetic electron scattering form factors of the ^{26}Mg nucleus. *Pramana – Journal of Physics* 2016; 86(1): 87–96.

http://doi.org/10.1007/s12043-015-1012-x.

Jassim KS, Faris AI. Nuclear structure of 60Ni nucleus using shell model calculations. *Journal of Computational and Theoretical Nanoscience* 2017; 14(5): 2336–2340.

http://doi.org/10.1166/jctn.2017.6830.

Bohr A, Mottelson BR. *Nuclear deformations.* WA Benjamin 1975.

Mottelson B. Nobel Prize lecture. *Reviews of Modern Physics* 1976; 48: 375.

De Forest Jr T, Walecka JD. Electron scattering and nuclear structure. *Advances in Physics* 1966; 15(57): 1-109.

Kumar K, Baranger M. Complete numerical solution of Bohr's collective Hamiltonian. *Nuclear Physics A* 1967; 92(3): 608-652.

Brussaard PJ, Glaudemans PWM, Glaudemans PWM. Shell-model applications in nuclear spectroscopy. *North-Holland publishing company* 1977.

Hynes MV, Miska H, Norum B, Bertozzi W, Kowalski S, Rad FN, Berman BL. Electron Scattering from the Ground-State Magnetization Distribution of 17O. *Physical Review Letters* 1979; 42(22): 1444–1448.

http://doi.org/10.1103/PhysRevLett.42.1444.

Kadhim AJ, Mohammed JH, Aljamali NM. Thiazole amide derivatives (Synthesis, spectral investigation, chemical properties, antifungal assay). *NeuroQuantology* 2020; 18(1): 16-25.

http://doi.org/10.14704/nq.2020.18.1.NQ20102

Négadi T. From RNA to the genetic code and back. *NeuroQuantology* 2020; 18(1): 1-7.

http://doi.org/10.14704/nq.2020.18.1.NQ19103